Virology 421 (2011) 96–104

Contents lists available at SciVerse ScienceDirect

Virology

journal homepage: www.elsevier.com/locate/yviro

Analyses of mutations selected by passaging a chimeric flavivirus identify mutations that alter infectivity and reveal an interaction between the structural proteins and the nonstructural glycoprotein NS1

Evandro R. Winkelmann [a], Douglas G. Widman [b,d], Ryosuke Suzuki [a,e], Peter W. Mason [a,b,c,f,*]

[a] Department of Pathology, University of Texas Medical Branch, Galveston, TX 77555-0436, USA
[b] Department of Microbiology and Immunology, University of Texas Medical Branch, Galveston, TX 77555-0436, USA
[c] Sealy Center for Vaccine Development, University of Texas Medical Branch, Galveston, TX 77555-0436, USA
[d] Lineberger Comprehensive Cancer Center, University of North Carolina, Chapel Hill, NC 27599-7295, USA
[e] National Institute of Infectious Diseases, Shinjuku-ku, Tokyo 162-8640, Japan
[f] Microbial Molecular Biology, Novartis Vaccines and Diagnostics, Cambridge, MA, 02139, USA

ARTICLE INFO

Article history:
Received 6 May 2011
Returned to author for revision 6 June 2011
Accepted 8 September 2011
Available online 13 October 2011

Keywords:
Flavivirus
Single-cycle virus
Chimera
RepliVAX
Packaging

ABSTRACT

We previously described a single-cycle dengue vaccine (RepliVAX D2) engineered from a capsid (C) gene-deleted West Nile virus (WNV) expressing dengue virus serotype 2 (DENV2) prM/E genes in place of the corresponding WNV genes. That work demonstrated that adaptation of RepliVAX D2 to grow in WNV C-expressing cells resulted in acquisition of non-synonymous mutations in the DENV2 prM/E and WNV NS2A/NS3 genes. Here we demonstrate that the prM/E mutations increase the specific infectivity of chimeric virions and the NS2A/NS3 mutations independently enhance packaging. Studies with the NS2A mutant demonstrated that it was unable to produce a larger form of NS1 (NS1'), suggesting that the mutation had been selected to eliminate a ribosomal frame-shift "slippage site" in NS2A. Evaluation of a synonymous mutation at this slippage site confirmed that genomes that failed to make NS1' were packaged more efficiently than WT genomes supporting a role for NS1/NS1' in orchestrating virion assembly.

Introduction

Flaviviruses are single-stranded, positive-sense RNA viruses and have an 11-kb genome with a single open reading frame encoding three structural proteins (C, prM/M and E) and seven non-structural proteins (NS1, NS2A, NS2B, NS3, NS4A, NS4B and NS5). Flavivirus RNA replication occurs in the cell cytoplasm via a negative-strand RNA intermediate, ultimately leading to the accumulation of positive-strand RNAs. Several NS proteins have been implicated in genome replication. The NS2B/NS3 serine protease is required for proteolytic processing at multiple sites in the viral polyprotein. NS3 also possesses RNA triphosphatase and RNA helicase activities and NS5 contains methyltransferase and RNA-dependent RNA polymerase activities (Lindenbach et al., 2007). NS1 is a non-structural glycoprotein that is secreted from mammalian but not insect cells infected by flaviviruses (Mason, 1989), and is found at high concentrations in the blood of viremic dengue patients (Alcon et al., 2002; Libraty et al., 2002).

NS1 is found in the viral polyprotein immediately following the two structural proteins, prM/E. The coding regions of these proteins are separated by signal peptidase cleavage sites, and all three proteins acquire N-linked carbohydrates during their synthesis (Lindenbach et al., 2007). prM and E form heterodimers which eventually undergo a complicated maturation process that produces E dimers that cover the surface of the mature viral particle (Li et al., 2008; Yu et al., 2008). Early studies demonstrated that NS1 was slowly secreted from mammalian cells, and studies with trans-expressed prM/E/NS1 cassettes suggested a role for NS1 in virion morphogenesis (Fan and Mason, 1990; Konishi et al., 1991; Mason, 1989). However, work with NS1 mutants demonstrated that NS1 played an essential role in viral RNA replication (Muylaert et al., 1996; Muylaert et al., 1997).

The insect-vectored flaviviruses are responsible for considerable morbidity and mortality worldwide. The viruses exist on all continents of the world except Antarctica, and threaten much of the world's population. DENV infections are estimated to occur in up to 100 million individuals annually and over 2.5 billion people live in areas at risk for DENV infection. Vaccines are available for a number of flavivirus diseases, including YF and JE, but there are currently no vaccines available for dengue. Among the marketed vaccines, the YF vaccine, which consists of the live-attenuated strain YF-17D, has been widely recommended to travelers, and has been considered to be remarkably safe and efficacious. However, recent documentation

* Corresponding author at: Novartis Vaccines and Diagnostics, Inc., 45 Sidney Street, Cambridge, MA 02139, USA.
E-mail address: peter.mason@novartis.com (P.W. Mason).

0042-6822/$ – see front matter © 2011 Elsevier Inc. All rights reserved.
doi:10.1016/j.virol.2011.09.007

of disease in a tiny fraction of those vaccinated with YF-17D prompted reconsideration of its safety and as a result, the American Committee on Immunization Practices now recommends that the risk of infection with YFV be taken into account when vaccinating travelers from non-endemic regions (Staples et al., 2010). Nevertheless, YF-17D continues to be an important public health tool, and has undisputable benefit in populations at high risk of YFV infection. In the case of JE vaccines, a live-attenuated vaccine is widely used in China, but safety and manufacturing issues have restricted it from being used in other regions of the world (Halstead and Thomas, 2011). In these areas, the product of choice was an efficacious inactivated mouse-brain derived virus, but safety concerns prompted its removal from use. However, new products, including cell-culture derived inactivated vaccines and a chimeric live-attenuated product based on YFV 17D are now being marketed in developed economies (Halstead and Thomas, 2011).

Recently, we reported the development of single-cycle flaviviruses that can be used as safe and effective vaccines (Mason et al., 2006). This single-cycle technology has been used to produce a series of vaccine candidates (named RepliVAX), that encode genomes harboring a truncated C (trC) gene that prevents the RepliVAX genome from being packaged into infectious particles unless the C gene is supplied in *trans* (Ishikawa et al., 2008; Mason et al., 2006; Suzuki et al., 2009; Widman et al., 2008). RepliVAX can infect normal cells in vaccinated animals, and these infected cells release prM/E-containing sub-viral particles (SVPs) and NS1 that induce effective antiviral immune responses. However, RepliVAX cannot spread or cause disease in animals, thus making them safe live-attenuated vaccines. The most recent addition to the RepliVAX family is a chimeric RepliVAX that expresses the prM/E genes of DENV2 in place of the WNV structural genes, and this vaccine (RepliVAX D2) was able to control DENV2 disease in a mouse model for DENV2 infection (Suzuki et al., 2009).

During our development of RepliVAX D2, we discovered that the initial construct grew poorly in C-expressing cells, but that growth could be improved by extensive blind passage (facilitated by introduction of larger fragments of the C gene and passaging of packaging cells along with the single-cycle virus). Analyses of these blind-passaged variants demonstrated that their improved growth characteristics were associated with the acquisition of specific mutations in the coding regions for prM, E, NS2A and NS3. In the case of the mutations in prM and E, we used reverse genetics to show that a pair of mutations in M (amino acid 9: G->R and amino acid 13: E->V; referred to by convention as $M^{R9G,V13E}$) and a single mutation in E (E^{K120T}; numbering convention as shown for M) both operated individually to increase yield of RepliVAX D2 in culture, but the combination of the M and E mutations worked together to produce the greatest enhancement in viral growth (Suzuki et al., 2009). Further, we showed that the mutations in the NS2A ($NS2A^{S9F}$) and the NS3 genes of the WNV backbone ($NS3^{R516K}$) enhanced growth of a re-engineered RepliVAX D2, but did not appear to have an effect on genome replication *per se*, since they were unable to enhance replication of WNV replicons that did not contain DENV genes (Suzuki et al., 2009).

Here we report that the mutations we identified in the growth-adapted chimeric RepliVAX D2 constructs in the DENV2 prM and E region improve specific infectivity of flavivirus particles in a manner similar to that of a previously characterized heparan sulfate (HS)-binding mutation at a nearby position in E (E^{K126E}) (Lee et al., 2006). In addition, we demonstrate that the mutation in the WNV NS2A (which acts in concert with the WNV NS3 mutation) eliminates the production of an altered form of NS1 (NS1') that arises from ribosome slippage at a site found in WNV, but not DENV (Firth and Atkins, 2009; Melian et al., 2010). Finally, we demonstrate that the elimination of the production of NS1' by introduction of a synonymous mutation in this ribosomal slippage site improved encapsidation of particles without altering the amplification and translation of the genome, indicating a functional interaction between NS1/NS1' and the structural proteins of flaviviruses during encapsidation.

Results

Mutations in DENV prM/E increase growth and alter specific infectivity

To determine how growth-enhancing mutations in the DENV2 prM/E coding region of single-cycle chimeric flaviviruses expressing the prM/E genes of DENV2 and the NS genes of WNV function (Suzuki et al., 2009), we produced a series of packaging cell lines (see Fig. 1A) that encoded the low passage DENV2 New Guinea C (NGC) prM/E sequences [BHK(VEErep/WNVC*-DENV2prM/E/Pac)] used to make our first generation RepliVAX D2 as well as a cell line [BHK(VEErep/WNVC*-DENV2pr/$M^{R9G,V13E}$/E^{K120T}/Pac)] that encoded the DENV2 prM/E sequences selected when RepliVAX D2 was adapted to grow in cells expressing the C gene (Suzuki et al., 2009). These packaging cells, along with cell lines carrying packaging constructs expressing the WNV prM/E [BHK(VEErep/WNVC*-E/Pac)], the JEV prM/E [BHK (VEErep/WNVC*-JEVprM/E/Pac)], and a cell line [BHK(pVEErep/WNVC*-DENV2prM/E^{K126E}/Pac] expressing an E protein from a high-passage NGC strain of DENV that contains a DENV2 E mutation (E^{K126E}) previously associated with HS binding (Lee et al., 2006) (see Fig. 1A) were used to produce viral replicon particles (VRPs) containing a WNV replicon (C-hFLuc2A-NS1-5, see Fig. 3A). When these VRPs, which contained identical WNV-derived replicons transpackaged in the different coats provided by their packaging cell lines (Fig. 1A), were tested side-by-side for their specific infectivities in Vero cells (genome copies per IU; see Materials and methods), we discovered that the VRPs packaged in WNV or JEV prM/E proteins exhibited significantly better specific infectivities (500 to 2000 genome copies per IU) than particles packaged in any of the DENV2 coats (50,000 to 200,000 genome copies per IU; Fig. 1B). Among the DENV2-packaged VRPs, the VRPs coated with the prM/E proteins of a low-passage NGC strain [from BHK(VEErep/WNVC*-DENV2prM/E/Pac)] displayed the poorest infectivity (over 200,000 genome equivalents per IU), and the particles packaged in coats containing the previously identified HS-binding mutation at position 126 (Lee et al., 2006) [BHK(pVEErep/WNVC*-DENV2prM/E^{K126E}/Pac)] displayed a slightly better specific infectivity. Interestingly, the VRPs packaged in the cell lines encoding the DENV2 prM/E genes selected in our RepliVAX D2 passaging studies (Suzuki et al., 2009) [BHK(VEErep/WNVC*-DENV2pr/$M^{R9G,V13E}$/E^{K120T}/Pac)] displayed a significantly better specific infectivity than the particles packaged in the WT DENV2-packaged VRPs, which contained the same low-passage DENV2 genes used to initiate the passaging studies we performed with RepliVAX D2 (Suzuki et al., 2009) (Fig. 1B). Taken together, these data demonstrate that the previously reported low-specific infectivity of DENV particles (van der Schaar et al., 2007) is due to the properties of the virion surface proteins and that changes in specific infectivity in cell culture can be facilitated by addition of positively charged residues in M and E that presumably function by facilitating productive binding of negatively charged glycosaminoglycans (GAGs) such as HS that are ubiquitously expressed on cells in culture and aid in infection as previously demonstrated for DENV2 (Lee et al., 2006). However, we cannot rule out the possibility that the mutations in prM/E could also have a role in the maturation of the structural proteins needed for flavivirus morphogenesis, especially in light of recent work showing that extracellular DENV particles contain a mixture of mature (lacking prM) and immature particles (Junjhon et al., 2010) which likely contribute to their poor specific infectivity.

NS2A and NS3 mutations previously selected in DENV2/WNV chimeras improve VRP growth when packaged in DENV2 envelopes

During propagation of a derivative of RepliVAX D2 containing the prM/E mutations described above (Suzuki et al., 2009), two mutations were selected in the WNV nonstructural protein-encoding regions that improved the growth of these chimeric viruses. To help learn how these mutations exerted their effects, we introduced

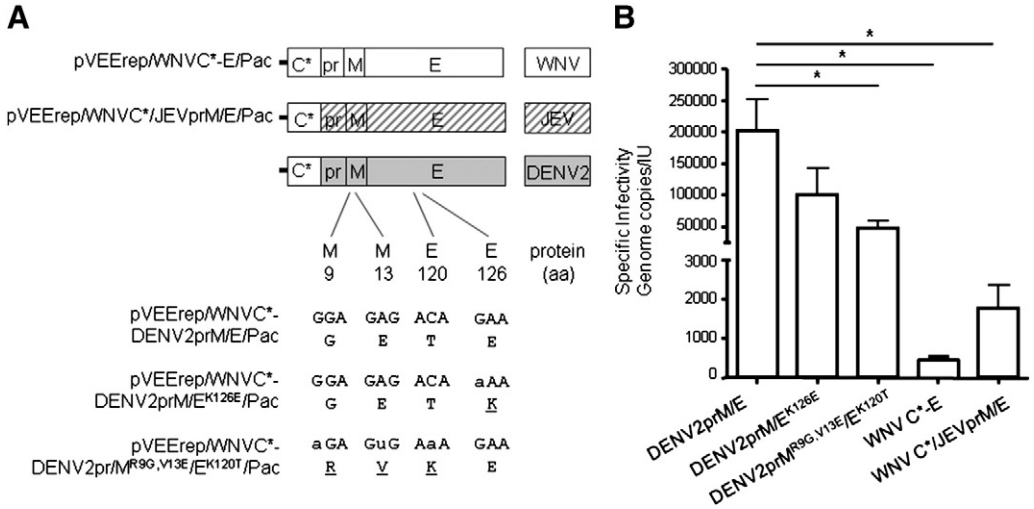

Fig. 1. Effect of flavivirus M/E proteins on the specific infectivity of trans-encapsidated WNV replicon genomes. (A) Schematic representation of the packaging cell constructs. All constructs contained a form of the WNV C protein (C*) engineered to contain synonymous mutations in the start of the genome to prevent generation of homologous recombinants with the replicons, as well as complete prM/E cassettes from the indicated viruses (see Materials and methods); "aa" indicates the position of the affected codon within the individual protein-coding regions. (B). Specific infectivities of VRPs created by packaging a WNV-derived replicon [pWNR C-hFLuc2A NS1-5-encoding hFLuc (see Materials and methods and Fig. 3A)]. Data displayed indicate the particle number (determined by genome quantification using sqPCR) divided by the measured infectivity on Vero cells (see Materials and methods). Error bars indicate the standard deviation between specific infectivity determinations established from two measurements of RNA concentration from the linear range of the sqPCR standard curve. "*" denotes significance as measured by one-way ANOVA with Bonferroni post-test ($p<0.05$).

them into RepliVAX WN (as single or double mutations; Fig. 2A), and tested how these mutations affected the growth of this non-chimeric single-cycle virus in a WNV C-expressing cell line [BHK(VEErep/Pac-Ubi-C*)]. Fig. 2B shows growth curves for the WT and mutated RepliVAX WN that were created by averaging values from 3 independent experiments. These growth curves demonstrate that the mutations selected in the context of the chimeric RepliVAX D2 were unable to produce a detectable improvement in growth of the non-chimeric RepliVAX WN.

To further evaluate the interactions between WNV NS2A and NS3 mutations and the DENV2 prM/E cassettes, NS2A^{S9F} and NS3^{R516K} were introduced as single- or double-mutations into a WNV replicon encoding a humanized form of the firefly luciferase (hFLuc) reporter gene (Fig. 3A). Comparison of the ability of VRPs containing these replicons to grow in a subset of the packaging cells described in Fig. 1 demonstrated that each of the non-structural protein mutations enhanced growth in all three of the DENV2 packaging cell lines (Figs. 3B, C and D). In addition, the two mutations displayed an additive/synergistic effect on transpackaging within DENV2 envelopes (Figs. 3B, C and D). However, neither of these mutations (independently or together) produced a detectable improvement in the growth of this WNV-derived replicon when replicons carrying these mutations were propagated in packaging cells expressing the WNV envelope protein cassette (Fig. 3E).

NS2A^{S9F} mutation alters the production of a higher molecular weight form of NS1

The recent observation that the NS2A gene of encephalitic flaviviruses contains a frame-shift motif (Firth and Atkins, 2009) that permits the production of an altered form of NS1 [known as NS1'; (Melian et al., 2010)] identified over 20 years ago in cells infected with JEV (Mason, 1989) prompted us to further examine our NS2A^{S9F} mutation. Interestingly, this mutation disrupts the canonical UUUU portion of the ribosome slip site that produces NS1' (CCCUUUU->CCCUUcU; Fig. 4A). To confirm that this mutation prevented the synthesis of NS1', we conducted Western blot analyses, that clearly demonstrate that this mutation results in the loss of NS1' (Fig. 4B).

Mutation of the ribosome slip site in NS2A enhances packaging of WN replicons in DENV2 coats and eliminates production of NS1'

To demonstrate that the growth enhancing properties of the NS2A^{S9F} mutation resulted through the abrogation of NS1' production, we engineered two silent mutations (CCCUUUU->CCC cUUc) in this region of NS2A (producing a construct designated NS2A^{F9F}) that disrupted the ribosome slip site (Fig. 5A). WNV replicons bearing this mutation alone, or in the presence of the NS3 mutation, displayed a significant enhancement of growth compared to the WT replicon genome when they were grown in cell lines providing DENV2 coats (Figs. 5B, C and D). Furthermore, Fig. 5E shows that the NS2A^{F9F} mutation, alone, or in concert with the NS3^{R516K} mutation produced a significant improvement in packaging in a WNV coat at several time points. As expected from the intentional disruption of the slippage site, cells infected with replicons expressing the NS2A^{F9F} mutation alone, or in the presence of the NS3^{R516K} mutation did not produce any detectable NS1' (Fig. 5F). To further understand the interaction between the NS2A^{F9F}and NS3^{R516K} mutations and DENV coats, we investigated the specific infectivity of C-hFLuc2A-NS1-5 and C-hFLuc2A-NS1-5 NS2A^{F9F} NS3^{R516K} VRPs produced in the WNVC*-DENV2pr/M^{R9G,V13E}/E^{K120T} and the WNVC*-E cell lines harvested from the 72 hpi time point in the study shown in Figs. 5D and E. These studies showed improved infectivity for the DENV-packaged VRPs that carried the NS2A frame-shift and NS3 mutations relative to the WT genomes, but no difference in the infectivity of the WNV-packaged genomes containing these mutations (Figs. S2A and B), suggesting that the C-hFLuc2A-NS1-5 NS2A^{F9F} NS3^{R516K} were more efficiently assembled into infectious DENV particles. Furthermore, Western blot analyses of the E protein content of these same VRP preparations showed a similar level of incorporation of WNV E into VRPs produced with either mutant or WT NS genes, but a more efficient incorporation of the DENV E into particles carrying the mutant NS genes, consistent with the hypothesis that the NS2A frame-shift and NS3 mutations produced higher infectious yields by increasing efficiency of assembly of infectious particles with DENV coats.

To further evaluate the role of these mutations in virion packaging in WNV coats, we utilized an additional, more sensitive assay consisting of calculating the size of infectious foci formed by VRPs carrying WT and mutant replicons on BHK(VEErep/WNVC*-E/Pac) cells.

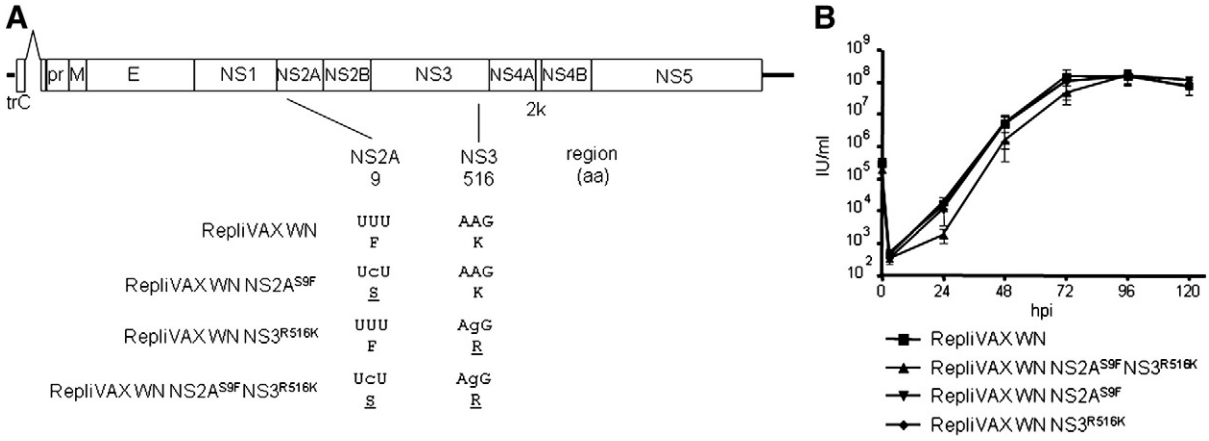

Fig. 2. NS2A^{S9F} and NS3^{R516K} mutations do not significantly improve the growth of RepliVAX derivatives carrying the WNV prM/E genes. (A) Schematic representation of derivatives of RepliVAX WN carrying mutations in NS2A and NS3; "aa" indicates the position of the affected codon within the individual protein-coding regions. (B) Growth curves of the RepliVAX WN constructs shown in Fig. 2A on BHK(VEErep/Pac-Ubi-C*) which express the WNV C protein. Cells were infected at an MOI of 0.01, and media were harvested, and titered at the indicated time points as described in the Materials and methods. The first time point (0 hpi) indicates the initial dose used to infect the cells. Values represent averages of three individual experiments. Error bars indicate standard deviation.

Fig. 6 shows the results of these assays, which support the data in Fig. 5E, by showing that all three VRPs tested in these assays tended to produce larger foci on cells expressing the WNV structural proteins.

NS1 is required for flavivirus genome replication, and mutations in NS1 have been shown to alter genome replication in cells in culture (see Introduction). To determine if the effect of NS1' abrogation was producing the enhanced growth/spread phenotype in packaging cell lines, we infected WT BHK cells with VRPs harboring various replicons and used the short-lived hFLuc reporter gene (Thompson et al., 1991) to quantify the levels of their genome replication and polyprotein translation. These studies, shown in Fig. 7, showed that neither the NS2A^{F9F}, NS3^{R516K}, nor the combined NS2A^{F9F}/NS3^{R516K} mutations significantly altered the levels of replicon amplification at 24 h post infection.

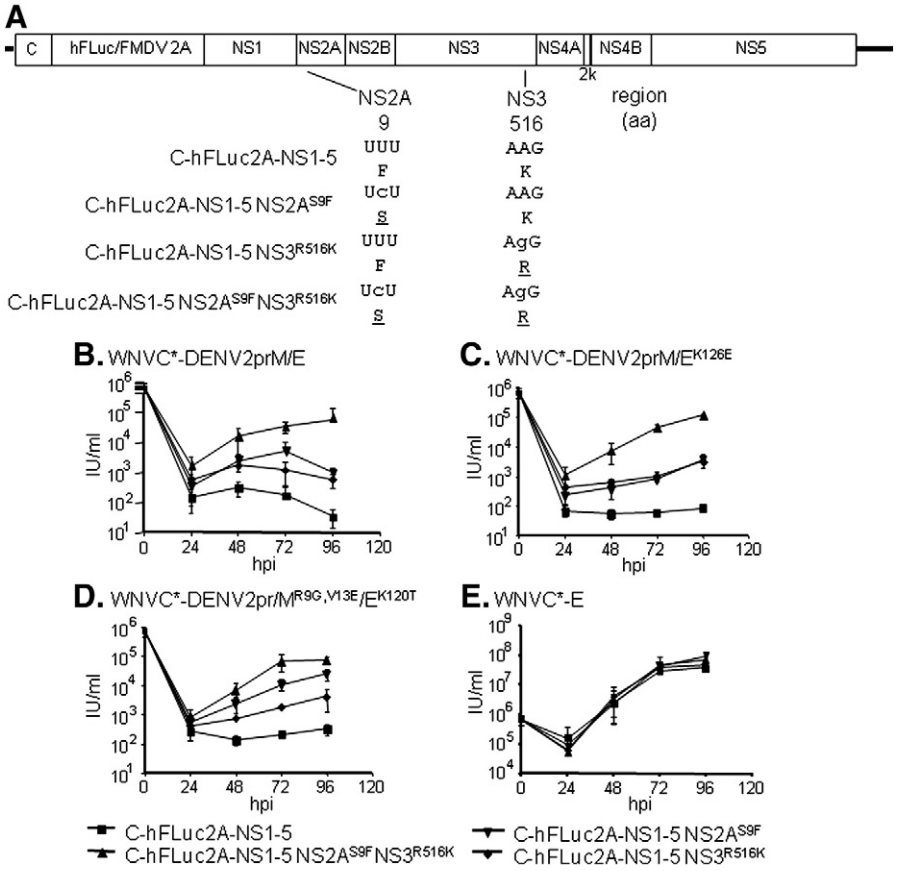

Fig. 3. NS2A^{S9F} and NS3^{R516K} improve growth of WNV VRPs when transpackaged in DENV coats. (A) Schematic representation of derivatives of WNV replicons carrying mutations in NS2A and NS3; "aa" indicates the position of the affected codon within the individual protein-coding regions. (B–E) Growth curves of VRPs harboring the genomes shown in Fig. 3A on BHK cell lines encoding the indicated packaging constructs. Cell monolayers were infected at an MOI of 0.05 with the indicated VRPs, and media were harvested and titered at the indicated time points as described in the Materials and methods. The first time point (0 hpi) indicates the initial dose used to infect the cells. Values represent averages of two individual experiments. Error bars indicate standard deviation.

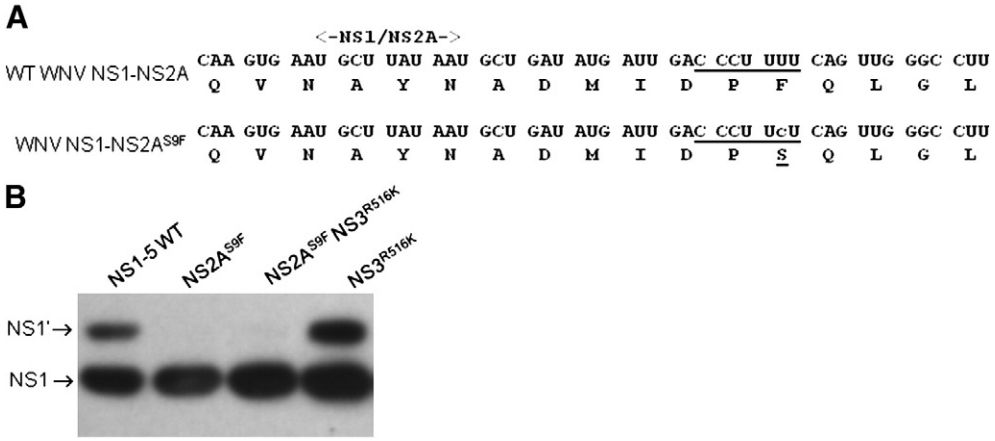

Fig. 4. Effect of NS2A^{S9F} mutation on synthesis of NS1'. (A) Alignment of RNA and amino acid sequences at the NS1/NS2A junction region of WNV showing the ribosomal frame-shift site (underlined) and its disruption by the NS2A^{S9F} mutation. (B) Western blot showing that cells infected with replicons encoding the NS2A^{S9F} mutation fail to produce NS1'. Cells infected with particles encoding C-hFLuc2A-NS1-5 replicon (labeled NS1-5 WT) and its derivatives (see Fig. 3A; labeled in this panel by mutation only) were lysed, blotted, and immunostained as described in the Materials and methods.

Discussion

Flaviviruses display a broad host- and cell-specificity which suggests that these viruses can use a variety of cell surface receptors. Multiple molecules have been identified that can serve as receptors, but the most clearly documented example of a cell-surface component that can be utilized as a receptor is the GAG, HS. Although the role of HS in natural infections by RNA viruses remains unclear, flaviviruses that are adapted to grow in cell culture or in specific animal models can acquire the ability to bind to HS through the acquisition of mutations on the E protein that produce positively charged patches that efficiently bind negatively charged GAGs (Anez et al., 2009; Kroschewski et al., 2003; Lee et al., 2004; Lee and Lobigs, 2000; Lee and Lobigs, 2002; Lee et al., 2006; Mandl et al., 2000). In the current studies we used a transpackaging system to demonstrate that the DENV2 M/E protein mutations found in our previously reported cell-adapted dengue chimera (Suzuki et al., 2009) improve the specific infectivity of transpackaged particles, explaining the selection of

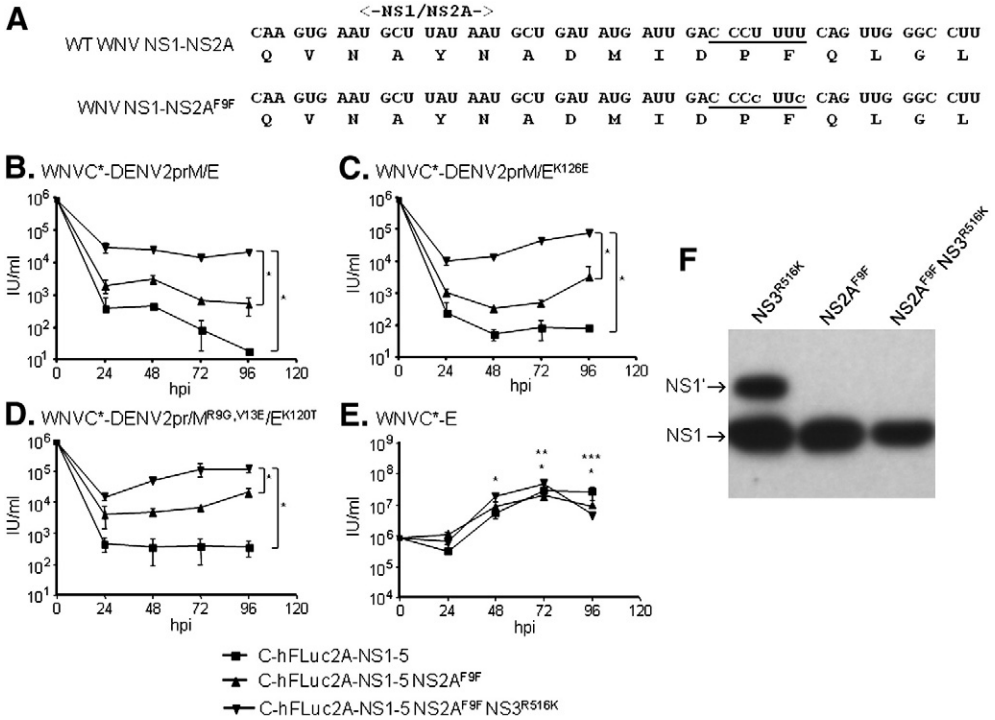

Fig. 5. Demonstration that ablation of ribosomal frame-shifting in NS2A enhances trans-encapsidation of WNV replicons and eliminates production of NS1'. (A) Alignment of RNA and amino acid sequences at the NS1/NS2A junction region of WNV showing the ribosomal frame-shift site (underlined) and its disruption by silent mutations. (B–E) Growth curves of VRPs harboring the WT replicon genomes, or genomes encoding the NS2A^{F9F} or NS2A^{F9F}NS3^{R516K} mutations on BHK cell lines encoding the indicated packaging constructs. Cell monolayers were infected at an MOI of 0.05 with the indicated VRPs, and media were harvested and titered at the indicated time points as described in the Materials and methods. The first time point (0 hpi) indicates the initial dose used to infect the cells. Values represent averages of two individual experiments. Error bars indicate standard deviation and "*" denotes significance as measured by two-way ANOVA with Bonferroni post-test ($p<0.05$) for 24–96 h timepoints (B and C) and 48–72 h timepoints (D). The same test showed significant differences in Fig. 5E; in this case: "*" denotes significance ($p<0.05$) for C-hFLuc2A-NS1-5 vs C-hFLuc2A-NS1-5NS2A^{F9F}NS3^{R516K}; "***" denotes significance ($p<0.05$) for C-hFLuc2A-NS1-5 NS2A^{F9F} vs C-hFLuc2A-NS1-5NS2A^{F9F}NS3^{R516K}; and "****" denotes significance ($p<0.05$) for C-hFLuc2A-NS1-5 vs C-hFLuc2A-NS1-5 NS2A^{F9F} at indicated timepoints. (F) Western blot showing that cells infected with VRPs containing the NS2A^{F9F} mutation fail to produce NS1'. Cells infected with particles encoding C-hFLuc2A-NS1-5 replicons encoding NS3^{R516K}, NS2A^{F9F}, or NS2A^{F9F} NS3^{R516K} mutations were lysed, blotted, and immunostained as described in the Materials and methods.

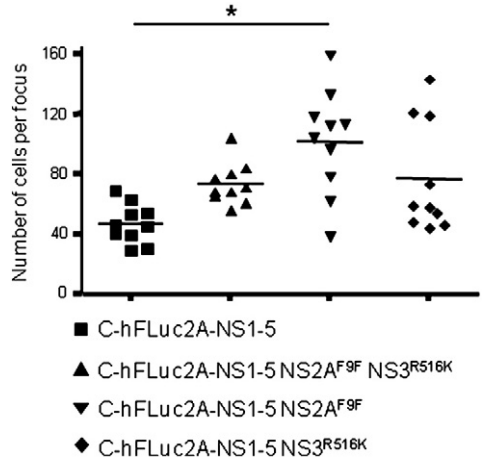

Fig. 6. Comparison of foci sizes of VRPs harboring the WT replicon genome, or genomes encoding the NS2A^{F9F}, NS2A^{F9F}NS3^{R516K} or NS3^{R516K} mutations on BHK(VEErep/WNVC*-E/Pac) cells expressing the WNV C-prM-E proteins. Cell monolayers were infected with serial dilutions of the VRPs, overlaid with semisolid medium, fixed, and immunostained with anti-NS1 antibody 48 h after incubation at 37 °C as described in the Materials and methods. The graph represents the counts of cells from 10 individual foci per VRP tested. The line represents the average of the 10 foci values for each group and "*" denotes significance as measured by one-way ANOVA with Bonferroni post-test ($p<0.001$).

these mutations during the adaptation of our dengue chimera to grow in cell culture. Furthermore, by comparing the specific infectivity of these preparations to those encoding envelopes of two encephalitic flaviviruses, we clearly demonstrated the poorer specific infectivity of particles encapsidated in DENV envelope proteins, consistent with work of Kuhn and co-workers documenting the poor specific infectivity of DENV2 virions (van der Schaar et al., 2007). Interaction among the proteins of positive-strand RNA viruses is one of the hallmarks of these viruses. Among the flaviviruses, numerous examples of such interactions exist within the structural proteins or within the well-defined non-structural protein complexes. Analyses of viable chimeras created from different species within the Flavivirus genus have revealed additional interactions. Several of these have documented interactions between components known to be involved in genome replication and the structural components of the virion. Among these, there has been a documented interaction of NS1 with the viral replicase via an interaction with NS4A (Lindenbach and Rice, 1999). In a previous report we demonstrated that adaptation of a DENV/WNV single-cycle chimeric flavivirus to grow to higher titers in a specifically designed packaging cell line resulted in the selection of mutations in NS2A and NS3. Here we definitively demonstrate that these mutations exert their growth-enhancing effect by interaction with the structural proteins, and that this growth enhancing effect is more pronounced in the context of DENV2 structural proteins. These data explain how these adaptations arose in response to the unnatural chimerization. In the case of the mutation in NS3, we were unable to define the mechanism by which this mutation was exerting its phenotype, but the ability of this mutation which lies within the helicase domain of NS3 to improve packaging of the viral genome supports previous evidence showing that changes in the helicase domain can alter encapsidation (Patkar and Kuhn, 2008).

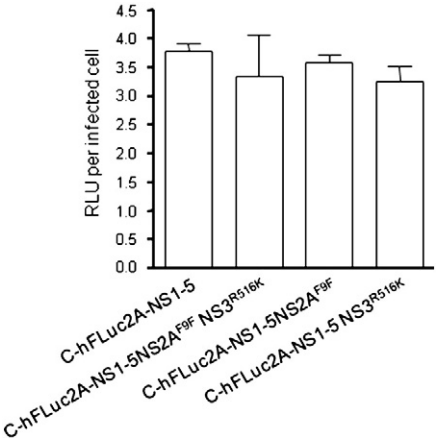

Fig. 7. Replication of VRPs harboring the WT replicon genome, or genomes encoding the NS2A^{F9F}, NS2A^{F9F}NS3^{R516K} or NS3^{R516K} mutations on BHK cells. Cells were cultured in 96-well plates, infected with VRPs and incubated for 24 h, when the relative luciferase units (RLU) were measured and then standardized to the number of VRP-infected cells obtained by immunostaining wells infected in a parallel plate (see Materials and methods). Data for each sample are averages of triplicate values with error bars showing standard deviations.

In the case of our NS2A mutation, which was found at codon 9 of the NS2A gene, we clearly demonstrate that this mutation functions through alteration of a recently documented ribosomal frame shift that produces an altered form of the NS1 protein (NS1') that is a characteristic of members of the JEV/WNV serocomplex of the flavivirus genus (Firth and Atkins, 2009; Mason, 1989; Melian et al., 2010). This interesting effect was evaluated by trans-complementation of genomes carrying the cell-adapted, non-synonymous mutation in NS2A which ablated the ribosome slippage site. These studies showed that this non-synonymous change increased transpackaging by prM/E proteins, and simultaneously eliminated the production of NS1'. The specific role of the frame shift in these phenotypes was confirmed by studies which demonstrated that synonymous mutations in this frame-shift site produced the same VRP growth-enhancing phenotype and ablation of NS1' production found in the non-synonymous mutation selected in our previous blind-passaging studies. Careful analyses of replicons harboring this mutation document that its effect on genome packaging, which was additive with the NS3 mutation, could be observed when packaging was evaluated in cells providing WNV or DENV2 prM/E coats. However, the growth-enhancing phenotype was more dramatic with the DENV2 prM/E coats, consistent with the hypothesis that these lower-specific infectivity coats provided a more significant selective pressure, allowing these mutations to arise in the chimeric background used for the initial passaging studies; the selection of these mutations is also consistent with preliminary studies showing that the combination of the NS2A frame-shift and NS3 point mutations into a replicon improve VRP yield from DENV E-producing cell lines by improving the specific infectivity of the resulting particles. Since the NS1 gene has been shown to serve a critical function in flavivirus genome replication we conducted studies to determine if ablation of NS1' by alteration of the slippage site could influence genome replication. These studies showed that abrogation of NS1' had no effect on genome replication, indicating that the mechanism by which NS1' alters particle packaging is due to an effect on virion assembly/release.

Our data demonstrating that the NS1' protein alters genome packaging expands the activities ascribed to the multifunctional NS1 protein. Although we have been unable to precisely determine how the larger form of the NS1 protein interferes with transpackaging of genomes into infectious particles, these findings are consistent with the slow egress of NS1 through the endoplasmatic reticulum (ER) of infected mammalian cells (Mason, 1989), the regulation of its localization to several compartments (Youn et al., 2010), the documented role of NS1 in genome replication (Muylaert et al., 1996; Muylaert et al., 1997), and interactions with NS4A (Lindenbach and Rice, 1999), all of which indicate that NS1 likely serves as a bridge between RNA synthesis and structural protein assembly. The finding that the extended form of NS1 has an inhibitory effect on virion packaging *in vitro* support this role. However, by themselves, these results are somewhat surprising. The fact that the effect on packaging was less pronounced in the presence of high-specific infectivity encephalitic flavivirus prM/E proteins is consistent with the fact that NS1' has

not been observed in other flaviviruses (see above). Interestingly, work by Khromykh and co-workers showed that abrogation of NS1' in a low-virulence isolate of WNV (Kunjin virus) reduced neurovirulence in mice (Melian et al., 2010). Although these studies did not document an effect of NS1' ablation on viral growth, they clearly showed an interesting effect of the NS1' protein *in vivo* but were unable to demonstrate any effect of the frame-shift ablation on growth of a mutant Kunjin virus *in vitro* in mammalian or insect cells (Melian et al., 2010). The inability to observe differences in growth of Kunjin viruses with or without the frame-shift mutation is consistent with our studies showing that productive growth of a single-cycle WNV (namely RepliVAX WN) in a complementing cell line was not improved by the introduction of this frame-shift mutation. Finally, although the influence of the frame shift on Kunjin virus neurovirulence may not provide an evolutionary advantage *per se*, the association of the frame-shift slippage site with the encephalitic flaviviruses likely reflects a selective biological advantage, which could be related to acquisition of additional functions by the larger form of NS1.

Materials and methods

Cells

BHK cells were maintained at 37 °C in minimal essential medium (MEM) supplemented with 10% fetal bovine serum (FBS) and antibiotics. Vero cells were maintained at 37 °C in MEM containing 6% FBS and antibiotics. BHK(VEErep/Pac-Ubi-C*) expressing the WNV C protein (Widman et al., 2008), BHK(VEErep/WNVC*-E/Pac) cells expressing the WNV C-prM-E proteins (Fayzulin et al., 2006), BHK(VEErep/WNC*-JEVprM-E/Pac) cells expressing the WNV C and JEV prM-E (Ishikawa et al., 2008), BHK(VEErep/WNVC*-DENV2prM/E/Pac) cells expressing the WNV C and the DENV2 NGC (low passage) prM/E (generated as described below), BHK(VEErep/WNVC*-DENV2prM/E^{K126E}/Pac) cells expressing the WNV C and a HS-binding E derived from a high-passage DENV2 NGC (generated as described below), and BHK(VEErep/WNVC*-DENV2pr/$M^{R9G,V13E}$/E^{K120T}/Pac) cells expressing the WNV C and the DENV2 prM/E mutations selected in RepliVAX D2 (generated as described below) were propagated at 37 °C in Dulbecco's MEM supplemented with 10% FBS and 10 μg/ml puromycin as previously described (Fayzulin et al., 2006).

Plasmid construction

The plasmid pWNR C-hFLuc2A NS1-5 encoding a WNV replicon expressing a hFLuc reporter gene has been previously described (Gilfoy et al., 2009). This was used to construct the various mutant WNV replicon plasmids with specific mutations in NS2A (pWNR C-hFLuc2A NS1-5 $NS2A^{S9F}$), NS3 (pWNR C-hFLuc2A CNS1-5 $NS3^{R516K}$), NS2A and NS3 (pWNR C-hFLuc2A NS1-5 $NS2A^{S9F}$/$NS3^{R516K}$), as well as a silent mutation in NS2A (pWNR C-hFLuc2A NS1-5 $NS2A^{F9F}$) using standard techniques (Higuchi et al., 1988).

The plasmid encoding the RepliVAX WN replicon [pRepliVAX WN (Widman et al., 2008); previously referred to as pRepliVAX WN.2 SP] was modified using standard techniques to produce a series of mutant RepliVAX WN plasmids with specific mutations in NS2A (pRepliVAX WN $NS2A^{S9F}$), NS3 (pRepliVAX WN $NS3^{R516K}$), and NS2A and NS3 (pRepliVAX WN $NS2A^{S9F}$/$NS3^{R516K}$) using standard techniques (Higuchi et al., 1988).

Plasmid pVEErep/WNVC*-E/Pac which encodes a Venezuelan equine encephalitis virus replicon (VEErep) capable of persisting in cells in the presence of puromycin and expressing the WNV structural proteins (C-prM-E) needed to package subgenomic replicons (Fayzulin et al., 2006) was used to construct a series of plasmids encoding a low-passage DENV2 NGC (Fonseca, 1994) prM/E cassette (pVEErep/WNVC*-DENV2prM/E/Pac), a high-passage DENV2 NGC (Fonseca, 1994) prM/E cassette (pVEErep/WNVC*-DENV2prM/E^{K126E}/Pac), or the prM/E cassette found in cell-adapted RepliVAX D2 (Suzuki et al., 2009) (pVEErep/WNVC*-DENV2pr/$M^{R9G,V13E}$/E^{K120T}/Pac). Sequences of all constructs are available from the authors upon request.

Production of packaging cell lines

Cell lines harboring replicons from the VEErep plasmids were created by a slight modification of the previously described procedures (Fayzulin et al., 2006). Briefly, the plasmid DNAs were linearized by using the MluI restriction enzyme, and the resulting template DNAs were *in vitro*-transcribed using MegaScript SP6 synthesis kit (Ambion) in the presence of 7mG(ppp)G cap analog (New England Biolabs). The yield and integrity of transcripts were determined by using non-denaturing gel electrophoresis, aliquots of transcription reactions were transfected into BHK cells using Lipofectin (Invitrogen), VEErep-harboring cell lines were selected in the presence of puromycin, and clones displaying high-level expression of these replicons were isolated and propagated using standard techniques.

Production of VRPs and RepliVAX WN derivatives

WNV replicon RNAs encoding the hFLuc gene (WNR C-hFLuc2A NS1-5 and derivatives) or the WNV prM/E cassette (RepliVAX WN and derivatives) were generated by using MegaScript T7 synthesis kit (Ambion) and 7mG(ppp)G cap analog (New England Biolabs) from SwaI-linearized templates created from the relevant plasmid DNAs using standard methods. Following analysis for yield and integrity as described above, aliquots of transcription reactions were electroporated into packaging cell lines (expressing C, prM, and E constructs in the case of the hFLuc-expressing replicon constructs or C only in the case of RepliVAX constructs) and then collected as previously described (Fayzulin et al., 2006).

VRP and RepliVAX titrations

VRPs and RepliVAX WN derivatives were titrated on Vero cells as previously described (Fayzulin et al., 2006). Yields are reported as infectious units per milliliter (IU/ml).

VRP and RepliVAX growth curves

To compare growth properties of the various WNV replicons in cell lines encoding various prM/E packaging constructs, VRPs derived from electroporations were used to infect these BHK packaging cells at a multiplicity of infection (MOI) of 0.05 for 2 h, the monolayers were washed 3 times (5 min each) with MEM supplemented with 1% FBS, 10 mM HEPES, and antibiotics, and the cultures were placed at 37 °C. Media were removed and replaced with fresh media at the indicated time points and stored at −80 °C for subsequent titration as described above.

Growth curves from RepliVAX WN and derivatives were prepared by infecting BHK(VEErep/Pac-Ubi-C*) cells at an MOI of 0.01 using the same procedure as described above.

Specific infectivity studies

Genome copy numbers and infectivity of VRPs produced by electroporation (see above) were determined based on semiquantitative PCR and Vero cell titration data. Briefly, VRP preparations were diluted to give titers of 1000 IU/ml, and one portion was titered on Vero cells as described above, while RNA was isolated from a second portion using the QIAamp Viral RNA kit (QIAGEN) following the manufacturer's protocol. The viral RNA concentration in this sample was determined by using a semiquantitative PCR (sqPCR) assay in which serial 2-fold dilutions of RNA from each sample were used for reverse transcription (RT) carried out with an ImProm II RT kit (Promega)

with random hexamers followed by amplification of a 100 bp PCR product using previously described WNV NS5-specific primers (Bourne et al., 2007). The PCR conditions included an initial cycle of 5 min at 95 °C, 30 cycles of 30 s at 95 °C, 30 s at 53 °C and 30 s at 72 °C, followed by 5 min at 72 °C. Following amplification, the PCR products were resolved by electrophoresis on 2% agarose gels containing 200 ng/ml of ethidium bromide, and images of the gels were acquired with a CCD camera using a FluorChem 8900 Chemiluminescence Gel Imager (Alpha Innotech) and band intensities were quantified by using ImageJ software (available at http://rsbweb.nih.gov/ij/). The intensities of these bands were compared to a standard curve generated with known numbers of genome copies of *in vitro* synthesized RNA from WNR C-hFLuc2A NS1-5 (ranging from 2000 to 200,000 copies), and the resulting standard curve (generated by using GraphPad Prism 4 software) (Fig. S1) was used to calculate the genome copies in each test sample. The specific infectivities of each preparation were then calculated by dividing this genome copy number per IU in the same sample volume, giving genome copies/IU of each VRP.

Western blot analyses of NS1

VRPs containing different derivatives of WNR C-hFLuc2A NS1-5 were inoculated onto BHK cell monolayers at an MOI of 5 and incubated at 37 °C with serum-free medium (OptiPro SFM, Gibco) supplemented with 10 mM HEPES and antibiotics. At 24 h after infection, culture fluids were collected and cell lysates were prepared using lysis buffer (0.1% Triton X-100, 300 mM NaCl, 50 mM Tris–HCl; pH 7.6) containing a protease inhibitor cocktail (Roche). Samples were resolved on 4–12% gradient Bis–Tris polyacrylamide gels (Invitrogen) and transferred to polyvinyldene diofluoride membranes, which were then incubated with a 1:5000 dilution of a mouse anti-NS1 antibody from hydridoma JE-6H4 (Kitai et al., 2007). Following washing, the membranes were incubated with a 1:10,000 dilution of peroxidase-conjugated anti-mouse IgG (KPL), and the bound peroxidase was visualized by using ECL Plus System (GE healthcare).

VRP focus-formation assay

To compare focus morphology, monolayers of BHK(VEErep/WNVC*-E/Pac) cells expressing the WNV C-prM-E proteins were infected with serial dilutions of VRPs harboring the WT replicon genome, or genomes encoding the NS2A^{F9F}, NS2A^{F9F}NS3^{R516K} or NS3^{R516K} mutations. Following absorption for 2 h, the cells were overlaid with medium containing 0.8% carboxymethyl cellulose (CMC) (Sigma, Saint Louis, MO) supplemented with 1% FBS, 10 mM HEPES and antibiotics and incubated at 37 °C for 48 h. To visualize foci, the cells were fixed with 50% acetone–50% methanol solution followed by incubation with a 1:5000 dilution of a mouse anti-NS1 antibody from hybridoma JE-6H4 (Kitai et al., 2007), peroxidase conjugated anti-mouse IgG (KPL, Gaithersburg, MD) and VIP substrate (Vector Laboratories, Burlingame, CA). The number of cells forming individualized focus was counted and used to compare focus size.

Luciferase assay

BHK monolayers prepared in 96-well black-wall plates were infected with dilutions of VRPs harboring the WT replicon genome, or genomes encoding the NS2A^{F9F}, NS2A^{F9F}NS3^{R516K} or NS3^{R516K} mutations and incubated at 37 °C. At 24 h post infection, an equal volume of 25% Steady-Glo Luciferase Assay System reagent (Promega) diluted in lysis buffer was added to the cells and incubated for 5 min on rocker to allow cell lysis. The luminescence was measured on a Microplate Luminometer (Applied Biosystems, Foster City, CA). A parallel plate infected with the same dilutions of VRPs was harvested at 24 h post infection and used to determine the number of VRP-infected cells determined by immunostaining (as described above). The luciferase activity was normalized by the number of VRP-infected cells and expressed as relative luciferase units (RLU) per infected cell.

Statistical analyses

GraphPad Prism (GraphPad Software, San Diego, CA) was used to analyze data. One-way or two-way analysis of variance (ANOVA) with the Bonferroni post-test were used where appropriate. P values less than 0.05 were considered to indicate statistical significance.

Acknowledgments

We thank T. Ishikawa (Kobe University) for helpful discussion concerning NS1' detection and E. Konishi (Kobe University) for supplying the JE-6H4 monoclonal antibody. This work was supported by a grant from NIAID to PWM through the Western Regional Center of Excellence for Biodefense and Emerging Infectious Disease Research (NIH grant number U54 AI057156), NIH grants R21 AI077077 and UO1 AI082960 and a grant from the Sealy Center for Vaccine Development (SCVD). ERW was supported by a SCVD Predoctoral Fellowship for a portion of these studies.

Appendix A. Supplementary data

Supplementary data to this article can be found online at doi:10.1016/j.virol.2011.09.007.

References

Alcon, S., Talarmin, A., Debruyne, M., Falconar, A., Deubel, V., Flamand, M., 2002. Enzyme-linked immunosorbent assay specific to Dengue virus type 1 nonstructural protein NS1 reveals circulation of the antigen in the blood during the acute phase of disease in patients experiencing primary or secondary infections. J. Clin. Microbiol. 40 (2), 376–381.

Anez, G., Men, R., Eckels, K.H., Lai, C.J., 2009. Passage of dengue virus type 4 vaccine candidates in fetal rhesus lung cells selects heparin-sensitive variants that result in loss of infectivity and immunogenicity in rhesus macaques. J. Virol. 83 (20), 10384–10394.

Bourne, N., Scholle, F., Silva, M.C., Rossi, S.L., Dewsbury, N., Judy, B., De Aguiar, J.B., Leon, M.A., Estes, D.M., Fayzulin, R., Mason, P.W., 2007. Early production of type I interferon during West Nile virus infection: role for lymphoid tissues in IRF3-independent interferon production. J. Virol. 81 (17), 9100–9108.

Fan, W.F., Mason, P.W., 1990. Membrane association and secretion of the Japanese encephalitis virus NS1 protein from cells expressing NS1 cDNA. Virology 177 (2), 470–476.

Fayzulin, R., Scholle, F., Petrakova, O., Frolov, I., Mason, P.W., 2006. Evaluation of replicative capacity and genetic stability of West Nile virus replicons using highly efficient packaging cell lines. Virology 351 (1), 196–209.

Firth, A.E., Atkins, J.F., 2009. A conserved predicted pseudoknot in the NS2A-encoding sequence of West Nile and Japanese encephalitis flaviviruses suggests NS1' may derive from ribosomal frameshifting. Virol. J. 6, 14.

Fonseca, B.A.L., 1994. Vaccinia-vectored dengue vaccine candidates elicit neutralizing antibodies in mice. Doctoral thesis. Yale University, New Haven, CT.

Gilfoy, F., Fayzulin, R., Mason, P.W., 2009. West Nile virus genome amplification requires the functional activities of the proteasome. Virology 385 (1), 74–84.

Halstead, S.B., Thomas, S.J., 2011. New Japanese encephalitis vaccines: alternatives to production in mouse brain. Expert Rev. Vaccines 10 (3), 355–364.

Higuchi, R., Krummel, B., Saiki, R.K., 1988. A general method of in vitro preparation and specific mutagenesis of DNA fragments: study of protein and DNA interactions. Nucleic Acids Res. 16 (15), 7351–7367.

Ishikawa, T., Widman, D.G., Bourne, N., Konishi, E., Mason, P.W., 2008. Construction and evaluation of a chimeric pseudoinfectious virus vaccine to prevent Japanese encephalitis. Vaccine 26 (22), 2772–2781.

Junjhon, J., Edwards, T.J., Utaipat, U., Bowman, V.D., Holdaway, H.A., Zhang, W., Keelapang, P., Puttikhunt, C., Perera, R., Chipman, P.R., Kasinrerk, W., Malasit, P., Kuhn, R.J., Sittisombut, N., 2010. Influence of pr-M cleavage on the heterogeneity of extracellular dengue virus particles. J. Virol. 84 (16), 8353–8358.

Kitai, Y., Shoda, M., Kondo, T., Konishi, E., 2007. Epitope-blocking enzyme-linked immunosorbent assay to differentiate West Nile virus from Japanese encephalitis virus infections in equine sera. Clin. Vaccine Immunol. 14 (8), 1024–1031.

Konishi, E., Pincus, S., Fonseca, B.A., Shope, R.E., Paoletti, E., Mason, P.W., 1991. Comparison of protective immunity elicited by recombinant vaccinia viruses that synthesize E or NS1 of Japanese encephalitis virus. Virology 185 (1), 401–410.

Kroschewski, H., Allison, S.L., Heinz, F.X., Mandl, C.W., 2003. Role of heparan sulfate for attachment and entry of tick-borne encephalitis virus. Virology 308 (1), 92–100.

Lee, E., Lobigs, M., 2000. Substitutions at the putative receptor-binding site of an encephalitic flavivirus alter virulence and host cell tropism and reveal a role for glycosaminoglycans in entry. J. Virol. 74 (19), 8867–8875.

Lee, E., Lobigs, M., 2002. Mechanism of virulence attenuation of glycosaminoglycan-binding variants of Japanese encephalitis virus and Murray Valley encephalitis virus. J. Virol. 76 (10), 4901–4911.
Lee, E., Hall, R.A., Lobigs, M., 2004. Common E protein determinants for attenuation of glycosaminoglycan-binding variants of Japanese encephalitis and West Nile viruses. J. Virol. 78 (15), 8271–8280.
Lee, E., Wright, P.J., Davidson, A., Lobigs, M., 2006. Virulence attenuation of Dengue virus due to augmented glycosaminoglycan-binding affinity and restriction in extraneural dissemination. J. Gen. Virol. 87 (Pt 10), 2791–2801.
Li, L., Lok, S.M., Yu, I.M., Zhang, Y., Kuhn, R.J., Chen, J., Rossmann, M.G., 2008. The flavivirus precursor membrane–envelope protein complex: structure and maturation. Science 319 (5871), 1830–1834.
Libraty, D.H., Young, P.R., Pickering, D., Endy, T.P., Kalayanarooj, S., Green, S., Vaughn, D.W., Nisalak, A., Ennis, F.A., Rothman, A.L., 2002. High circulating levels of the dengue virus nonstructural protein NS1 early in dengue illness correlate with the development of dengue hemorrhagic fever. J. Infect. Dis. 186 (8), 1165–1168.
Lindenbach, B.D., Rice, C.M., 1999. Genetic interaction of flavivirus nonstructural proteins NS1 and NS4A as a determinant of replicase function. J. Virol. 73 (6), 4611–4621.
Lindenbach, B.D., Theil, H.-J., Rice, C.M., 2007. *Flaviviridae*: the viruses and their replication, In: Knipe, D.M., Howley, P.M. (Eds.), Fifth ed. Fields Virology, Vol. 1. Lippincott Williams & Wilkins, Philadelphia, pp. 1101–1152. 2 vols.
Mandl, C.W., Allison, S.L., Holzmann, H., Meixner, T., Heinz, F.X., 2000. Attenuation of tick-borne encephalitis virus by structure-based site-specific mutagenesis of a putative flavivirus receptor binding site. J. Virol. 74 (20), 9601–9609.
Mason, P.W., 1989. Maturation of Japanese encephalitis virus glycoproteins produced by infected mammalian and mosquito cells. Virology 169 (2), 354–364.
Mason, P.W., Shustov, A.V., Frolov, I., 2006. Production and characterization of vaccines based on flaviviruses defective in replication. Virology 351 (2), 432–443.
Melian, E.B., Hinzman, E., Nagasaki, T., Firth, A.E., Wills, N.M., Nouwens, A.S., Blitvich, B.J., Leung, J., Funk, A., Atkins, J.F., Hall, R., Khromykh, A.A., 2010. NS1' of flaviviruses in the Japanese encephalitis virus serogroup is a product of ribosomal frameshifting and plays a role in viral neuroinvasiveness. J. Virol. 84 (3), 1641–1647.
Muylaert, I.R., Chambers, T.J., Galler, R., Rice, C.M., 1996. Mutagenesis of the N-linked glycosylation sites of the yellow fever virus NS1 protein: effects on virus replication and mouse neurovirulence. Virology 222 (1), 159–168.
Muylaert, I.R., Galler, R., Rice, C.M., 1997. Genetic analysis of the yellow fever virus NS1 protein: identification of a temperature-sensitive mutation which blocks RNA accumulation. J. Virol. 71 (1), 291–298.
Patkar, C.G., Kuhn, R.J., 2008. Yellow Fever virus NS3 plays an essential role in virus assembly independent of its known enzymatic functions. J. Virol. 82 (7), 3342–3352.
Staples, J.E., Gershman, M., Fischer, M., 2010. Yellow fever vaccine: recommendations of the Advisory Committee on Immunization Practices (ACIP). MMWR Recomm. Rep. 59 (RR-7), 1–27.
Suzuki, R., Winkelmann, E.R., Mason, P.W., 2009. Construction and characterization of a single-cycle chimeric flavivirus vaccine candidate that protects mice against lethal challenge with dengue virus type 2. J. Virol. 83 (4), 1870–1880.
Thompson, J.F., Hayes, L.S., Lloyd, D.B., 1991. Modulation of firefly luciferase stability and impact on studies of gene regulation. Gene 103 (2), 171–177.
van der Schaar, H.M., Rust, M.J., Waarts, B.L., van der Ende-Metselaar, H., Kuhn, R.J., Wilschut, J., Zhuang, X., Smit, J.M., 2007. Characterization of the early events in dengue virus cell entry by biochemical assays and single-virus tracking. J. Virol. 81 (21), 12019–12028.
Widman, D.G., Ishikawa, T., Fayzulin, R., Bourne, N., Mason, P.W., 2008. Construction and characterization of a second-generation pseudoinfectious West Nile virus vaccine propagated using a new cultivation system. Vaccine 26 (22), 2762–2771.
Youn, S., Cho, H., Fremont, D.H., Diamond, M.S., 2010. A short N-terminal peptide motif on flavivirus nonstructural protein NS1 modulates cellular targeting and immune recognition. J. Virol. 84 (18), 9516–9532.
Yu, I.M., Zhang, W., Holdaway, H.A., Li, L., Kostyuchenko, V.A., Chipman, P.R., Kuhn, R.J., Rossmann, M.G., Chen, J., 2008. Structure of the immature dengue virus at low pH primes proteolytic maturation. Science 319 (5871), 1834–1837.